British Journal of Mathematics & Computer Science
15(1): 1-14, 2016, Article no.BJMCS.23222
ISSN: 2231-0851

SCIENCEDOMAIN *international*
www.sciencedomain.org

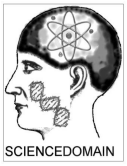

Oscillatory Blood Flow in Convergent and Divergent Channels, Part 2: Effects of Reynolds Number

W. I. A. Okuyade[1*] and T. M. Abbey[2]

[1]Department of Mathematics, University of Port Harcourt, Port Harcourt, Nigeria.
[2]Department of Physics, Applied Mathematics and Theoretical Physics Group, University of Port Harcourt, Port Harcourt, Nigeria.

Authors' contributions

This work was carried out in collaboration between authors WIAO and TMA. Author TMA designed the study, wrote the protocol and supervised the work. Author WIAO wrote the introduction and solved the problem under the guidance of author TMA. Author TMA did the programming for the results while author WIAO managed the analyses of the study. Author WIAO wrote the first draft of the manuscript, managed the literature searches and edited the manuscript. Both authors read and approved the final manuscript.

Article Information

DOI: 10.9734/BJMCS/2016/23222
Editor(s):
(1) Kai-Long Hsiao, Taiwan Shoufu University, Taiwan.
Reviewers:
(1) J. Prakash, University of Botswana, Botswana.
(2) John Abraham, University of St. Thomas, Minnesota, USA.
(3) Nityanand P. Pai, Manipal University, India.
Complete Peer review History: http://sciencedomain.org/review-history/13476

Original Research Article

Received: 21st November 2015
Accepted: 30th December 2015
Published: 27th February 2016

Abstract

This paper studies the effects of Reynolds number on the oscillating flow in convergent and divergent channels. The nonlinear equations governing the flow are solved analytically by the method of perturbation series solutions. Expressions for the velocities and wall shear stress are obtained and analyzed graphically. It is found that increase in the Reynolds number increases the velocities and wall shear stress. Similarly, it is seen that a flow separation occurs in the radial velocity flow structure.

Keywords: Convergent and divergent channels; oscillatory flow; perturbation method.

**Corresponding author: E-mail: wiaokuyade@gmail.com, tamunoimi.abbey@uniport.edu.ng;*

1 Introduction

The human artery is infested by a number of diseases. Amongst these is atherosclerosis, which involves the hardening of the artery due to deposition of lipids (a generic name for esters) on its internal walls. The calcification of the lipids at the points of infection leads to lose of distensibility at such points. Also, the progressive encroachment of the plague on its internal walls tends to block the passage of blood to other parts of the body. And, this imposes extra loads on the heart musculature. To maintain the peripheral flow, the heart enlarges itself, and thus, increasing the amplitude of the pulse or pressure wave. More so, the encroachment of the plague which may overlap leads to distortion of the tapered geometry of the artery to other forms, such as the idealized locally constricted and peristaltic geometries.

[1] investigated the fluid mechanical aspect of the pulsatile flow of an incompressible fluid through a tapered, locally constricted and peristaltic channels. Their model did not consider the flow behavior in the regions before and after the peak of the stenos height, which are idealized as the convergent and divergent channels. Therefore, we are motivated to examine the flow behaviour in the convergent and divergent channels using the same problem.

In part one of these studies, the effect of variations in the pressure wave amplitude and height of constriction on the flow structures of blood in the region before and after the critical height of the constriction, approximated by the convergent and divergent channels were examined. The study did not consider the effects of Reynolds number on the flow. Therefore, in this model we shall investigate the effects of Reynolds number on the flow.

Some work exists in literature on the flow of an incompressible and viscous fluid in channels of varying cross-sections. For example, [1] considered the pulsating flow of a Newtonian, and incompressible viscous fluid in channels of varying cross-session using the perturbation series expansion solutions which they developed, and observed that flow separation occurs in all geometries; [2,3,4] and [5] studied the flow in locally constricted and peristaltic channels; [6] solved the Navier–Stokes and the energy equations by the method of finite difference, and noticed the existence of an annular effect in the entry region for the pulsatile part of the velocity and temperature; [7] solved the Navier–Stokes and energy equations numerically for the laminar pulsating flow in a channel, and concluded that an appreciable heat transfer enhancement occurs in the channel. Furthermore, [8] studied the unsteady three-dimensional fluid mechanics analysis of blood flow in a plagued artery with the aim of quantifying the effectiveness of plague removal modalities in the small arteries using the method of numerical simulation, and observed that the removal of the plague leads to an increase in the flow rate of blood during the systole and diastole portions of the cardiac cycle; [9] investigated a time-wise periodic pipe flow using numerical simulation approach, and identified a large-periodic limit at which the flow is quasi-steady. More so, [10] considered the time-varying pipe flow driven by a harmonically pulsating inlet velocity using the Mente transitional numerical simulation model, and observed that the use of quasi-steady model for predicting the fully developed friction factor is not applicable to higher frequency. They also noticed that backflow occurs near the walls as the flow transits from deceleration to acceleration. Even so, [11] examined the influence of heat and chemical reactions on blood flow through an anisotropically tapered and elastic artery with overlapping stenosis, and found among others, that the coupling number, tapering angle, maximum height of stenosis, Sorret number and Brinkman number tend to increase the axial velocity higher for the Newtonian fluid than for the micro-polar fluid; [12] considered the MHD flow of an incompressible viscous fluid through convergent and divergent channels using the homotopy perturbation method, and noticed that the behaviour of the homotopy perturbatiom method is in good agreement with the numerical simulations.

This paper presents an analytic model on the effect of Reynolds number on the velocity and wall shear stress structures of the oscillatory flow in convergent and divergent tubes.

The paper is organized in the following format: section 2 gives the methodology; section 3 holds the results and discussion, while section 4 presents the conclusions.

2 Methodology

The problem examined the flow of blood in axi-symmetric convergent and divergent channels. These channels approximate the region before and after the critical point of the constriction caused by the stenosis of the artery. Due to the plague, the region of the artery affected becomes rigid and therefore, loses its distensibility. Let (R, θ, X) and (u,v,w) be the polar cylindrical orthogonal coordinates and vector components, respectively, and assuming the flow is symmetrical about the θ- axis, then for a two-dimensional situation, the coordinates and vector components are reduced to (R, 0, X) and (u, 0, w) respectively, such that the continuity, momentum and energy equations governing the flow become:

$$\frac{1}{R}\frac{\partial u}{\partial R}+\frac{\partial u}{\partial R}+\frac{\partial u}{\partial X}=0 \tag{1}$$

$$\frac{\partial u}{\partial t}+u\frac{\partial u}{\partial R}+w\frac{\partial u}{\partial X}=-\frac{\partial p}{\partial R}+\upsilon\left(\frac{\partial^2 u}{\partial R^2}+\frac{1}{R}\frac{\partial u}{\partial R}-\frac{u}{R^2}+\frac{\partial^2 u}{\partial X^2}\right) \tag{2}$$

$$\frac{\partial w}{\partial \mathrm{t}}+\mathrm{u}\frac{\partial w}{\partial R}+w\frac{\partial w}{\partial X}=-\frac{1}{\rho}\frac{\partial \mathrm{p}}{\partial X}+\upsilon\left(\frac{\partial^2 w}{\partial \mathrm{R}^2}+\frac{1}{\mathrm{R}}\frac{\partial w}{\partial \mathrm{R}}+\frac{\partial^2 w}{\partial \mathrm{X}^2}\right) \tag{3}$$

where ρ the density, p the pressure, υ the kinematic viscosity of the fluid, and t is the time. R=0 is the centre or symmetric axis of the tube; $R=a_o(X,t)$, which is an arbitrary function of X and t is the cross-sectional radius of the tube; a_o is the characteristic radius of the tube, and t is the time.

The boundary conditions are:

(i) $\mathrm{w}=0,\ \dfrac{\partial u}{\partial \mathrm{R}}=0$ at R=0 (4)

(ii) by the no-slip condition at the wall of the tube

$$u(a_o,t)=0 \quad \text{at} \quad R=a_o(X,t) \tag{5}$$

(iii) the flux across a cross–section of the tube is prescribed as:

$$\int_0^{a_o(X,t)} dR \int_0^{2\pi} Ru\,d\theta = 2\,\pi\psi_o\,(1+k\,e^{\,i\beta t}) \tag{6}$$

where ψ_o is a constant, k is the amplitude of the pulse which is assumed to be small, and β is the frequency of oscillation.

To eliminate the pressure terms in equations (2) and (3) we take the partial derivatives of equations (2) and (3) with respect to R and X respectively, then subtracting the first result from the second one, we have

$$\frac{\partial}{\partial t}\left(\frac{\partial u}{\partial R}-\frac{\partial w}{\partial X}\right)+\frac{\partial u}{\partial X}\left(\frac{\partial u}{\partial R}-\frac{\partial w}{\partial X}\right)+\frac{\partial w}{\partial R}\left(\frac{\partial u}{\partial R}-\frac{\partial w}{\partial X}\right)=$$

$$\upsilon\left[\frac{\partial^2}{\partial X^2}\left(\frac{\partial u}{\partial R}-\frac{\partial w}{\partial X}\right)+\frac{\partial^2}{\partial R^2}\left(\frac{\partial u}{\partial R}-\frac{\partial w}{\partial X}\right)+\frac{1}{R}\frac{\partial}{\partial R}\left(\frac{\partial u}{\partial R}-\frac{\partial w}{\partial X}\right)-\frac{1}{R^2}\left(\frac{\partial u}{\partial R}-\frac{\partial w}{\partial X}\right)\right] \tag{7}$$

Also, the pressure expression in the axial direction can be obtained from equation (3), as

$$\frac{\partial p}{\partial X}=\upsilon\left(\frac{\partial^2 w}{\partial R^2}+\frac{1}{R}\frac{\partial w}{\partial R^2}+\frac{\partial^2 w}{\partial X^2}\right)-\left(\frac{\partial w}{\partial t}+u\frac{\partial w}{\partial R}+w\frac{\partial w}{\partial X}\right) \tag{8}$$

Introducing the stream function ψ, vorticity Ω, and non-dimensionalized variables, respectively, into equations (7) and (8), we have

$$u=-\frac{1}{r}\frac{\partial \phi}{\partial \mathrm{r}} \tag{9}$$

$$w=-\frac{1}{r}\frac{\partial \phi}{\partial \mathrm{x}} \tag{10}$$

$$\omega=\frac{1}{r}\frac{\partial^2 \phi}{\partial r^2}-\frac{1}{r^2}\frac{\partial \phi}{\partial r} \tag{11}$$

$$\eta\frac{\partial \omega}{\partial T}+\frac{\mathrm{Re}}{r}\varepsilon\left(\frac{\partial \omega}{\partial r}\frac{\partial \phi}{\partial x}+\frac{\partial \omega}{\partial x}\frac{\partial \phi}{\partial r}+\frac{\omega}{r}\frac{\partial \phi}{\partial x}\right)=\frac{1}{r^2}\frac{\partial^2 \omega}{\partial r^2}+\frac{1}{r}\frac{\partial \omega}{\partial r}-\frac{1}{r}\omega \tag{12}$$

$$\frac{\partial p}{\partial X}=-\frac{\mathrm{Re}}{\varepsilon}\left(-\frac{1}{r}\frac{\partial^3 \phi}{\partial r^3}+\frac{1}{r^2}\frac{\partial^2 \phi}{\partial r^2}\right)+\frac{\eta}{\varepsilon r}\frac{\partial^2 \phi}{\partial r \partial T} \tag{13}$$

Equation (13) shows that the pressure field is of order $\frac{1}{\varepsilon}$. Also, the O $(\varepsilon)^2$ terms are neglected for being small.

Furthermore, the wall shear stress is expressed as

$\tau_w=\rho \upsilon \Omega$ (see [5]) giving us

$$\tau_w=\frac{1}{r}\frac{\partial^2 \phi}{\partial r^2}+\frac{1}{r^2}\frac{\partial \phi}{\partial r} \tag{14}$$

The boundary conditions become:

$$\phi = 0 \ , \ \frac{\partial \phi}{\partial x} = 0 \ , \ \frac{\partial}{\partial \mathrm{r}}\left(\frac{1}{\mathrm{r}}\frac{\partial \phi}{\partial \mathrm{r}}\right) = 0 \quad \text{at} \quad \mathrm{r} = 0 \qquad (15)$$

$$\phi = 1 \ + \ \mathrm{k}\, \mathrm{e}^{\,\mathrm{iT}}, \ \frac{\partial \phi}{\partial \mathrm{r}} = 0 \quad \text{at} \quad \mathrm{r} = \mathrm{s}(\mathrm{x}, \mathrm{T}) \qquad (16)$$

Where

$$\mathrm{u} = -\frac{1}{R}\frac{\partial \psi}{\partial R}, \ \mathrm{w} = \frac{1}{\mathrm{R}}\frac{\partial \psi}{\partial X} \qquad (17)$$

$$\Omega = \frac{\partial u}{\partial R} - \frac{\partial w}{\partial X} = \frac{1}{\mathrm{R}}\frac{\partial^2 \psi}{\partial R^2} - \frac{1}{R^2}\frac{\partial \psi}{\partial R} + \frac{1}{R}\ \frac{\partial^2 \psi}{\partial \mathrm{X}^2} \qquad (18)$$

are the stream functions and vortices terms, and

$$r = \frac{R}{a_o} \ , x = \varepsilon \frac{X}{a_o}, \ \ \mathrm{T} \ = \ \beta \mathrm{t}, \ \ \phi \ (r, x, T) = \frac{\psi}{\psi_{\mathrm{o}}},$$

$$\omega(r, x, T) = \frac{\Omega \mathrm{a}_{\mathrm{o}}^3}{\psi_{\mathrm{o}}}, \mathrm{Re} = \frac{\psi_{\mathrm{o}}}{\mathrm{a}_{\mathrm{o}} \upsilon}, \ \eta \ = \frac{\beta}{a_o^2 \upsilon}, \ \mathrm{a}_{\mathrm{o}} = \frac{\mathrm{a}}{\mathrm{s}}$$

are the non-dimensionalized variables, where Re is the Reynolds number of the flow, η is a dimensionless number for the frequency of oscillation, T is the dimensionless time, ε is the height of constriction, ϕ, ω are the dimensionless stream function and vorticity, respectively. Also, we assume that the cross–section of the tube in the model vary in the axial direction, and for which we take a(X, t) = $a_o s$ (ε X/a_o , t) , $r = R_0(1 + \varepsilon f(x,t))$, 0 ≤ r ≤1, 0 ≤ x ≤1 where s is an arbitrary function of X; a is the variation in the r along the axial direction; $0 < \varepsilon = \frac{a_o}{L} << 1$ is a small dimensionless parameter that characterizes the slow variation in the channel radius; L defines the channel characteristic length. $\varepsilon = 0$ corresponds to a tube with constant radius. As ε increases from zero the variation of ψ in the axial direction depends upon ε X instead of X.

We shall seek for perturbation series solutions about the small parameter ε of the form:

$$f \ = \ f^{(o)} + k e^{iT}\, \overline{f}^{(o)} + \varepsilon \left(f^{(1)} + k e^{iT}\, \overline{f}^{(1)} \right) + \ldots \qquad (19)$$

where f_n represents ω and ϕ. This enables us to linearize the problems and make them tractable.

Therefore, substituting equation (19) into equations (11), (12), (15) and (16), we have the zeroth order terms as

$$\omega^{(o)} = \frac{1}{r}\left(\frac{\partial^2\phi^{(o)}}{\partial r^2} - \frac{1}{r}\frac{\partial\phi^{(o)}}{\partial r}\right) \tag{20}$$

$$\omega^{(o)} = \frac{1}{r}\left(\frac{\partial^2\bar{\phi}^{(o)}}{\partial r^2} + \frac{1}{r}\frac{\partial\bar{\phi}^{(o)}}{\partial r}\right) \tag{21}$$

$$\frac{\partial^2\omega^{(o)}}{\partial r^2} + \frac{1}{r}\frac{\partial\omega^{(o)}}{\partial r} - \frac{1}{r^2}\ \omega^{(o)} = 0 \tag{22}$$

$$\frac{\partial^2\varpi^{(o)}}{\partial r^2} + \frac{1}{r}\frac{\partial\varpi^{(o)}}{\partial r} - \left(\lambda^2 + \frac{1}{r}\right)\varpi^{(o)} = 0 \tag{23}$$

where $\lambda^2 = i\eta$

with the boundary conditions

$$\left.\begin{aligned} &\phi^{(o)} = \bar{\phi}^{(o)} = 0 \\ &\frac{1}{r}\frac{\partial\phi^{(o)}}{\partial x} = \frac{1}{r}\frac{\partial\bar{\phi}^{(o)}}{\partial x} = 0 \\ &\frac{\partial}{\partial r}\left(\frac{1}{r}\frac{\partial\phi^{(o)}}{\partial r}\right) = \frac{\partial}{\partial r}\left(\frac{1}{r}\frac{\partial\bar{\phi}^{(o)}}{\partial r}\right) = 0 \end{aligned}\right\} \text{ at } r = 0 \tag{24}$$

$$\left.\begin{aligned} &\frac{\partial\phi^{(o)}}{\partial r} = \frac{\partial\bar{\phi}^{(o)}}{\partial r} = 0 \\ &\phi^{(o)} = \bar{\phi}^{(o)} = 1 \end{aligned}\right\} \quad \text{at} \quad r = s \tag{25}$$

and the first order terms

$$\omega^{(1)} = \frac{1}{r}\left(\frac{\partial^2\phi^{(1)}}{\partial r^2} - \frac{1}{r}\frac{\partial\phi^{(1)}}{\partial r}\right) \tag{26}$$

$$\varpi^{(1)} = \frac{1}{r}\left(\frac{\partial^2\bar{\phi}^{(1)}}{\partial r^2} - \frac{1}{r}\frac{\partial\bar{\phi}^{(1)}}{\partial r}\right) \tag{27}$$

$$\frac{\partial^2 \omega^{(1)}}{\partial r^2} + \frac{1}{r}\frac{\partial \omega^{(1)}}{\partial r} - \frac{1}{r}\ \omega^{(1)} = \frac{\mathrm{Re}}{r}\left[\frac{\partial \phi^{(o)}}{\partial r}\frac{\partial \omega^{(o)}}{\partial x} + \frac{\partial \phi^{(o)}}{\partial x}\left(\frac{\omega^{(o)}}{r} - \frac{\partial \omega^{(o)}}{\partial r}\right)\right] \tag{28}$$

$$\frac{\partial^2 \varpi^{(1)}}{\partial r^2} + \frac{1}{r}\frac{\partial \varpi^{(1)}}{\partial r} - \left(\lambda^2 + \frac{1}{r^2}\right)\varpi^{(1)} = \frac{\mathrm{Re}}{r}\left[\frac{\partial \phi^{(o)}}{\partial r}\frac{\partial \omega^{(o)}}{\partial x} + \frac{\partial \bar{\phi}^{(o)}}{\partial r}\frac{\partial \omega^{(o)}}{\partial x}\right.$$

$$\left. - \frac{\partial \varpi^{(o)}}{\partial x}\left(\frac{\partial \varpi^{(o)}}{\partial r} - \frac{\varpi^{(o)}}{r}\right) - \frac{\partial \bar{\phi}^{(o)}}{\partial x}\left(\frac{\partial \omega^{(o)}}{\partial r} - \frac{\omega^{(o)}}{r}\right)\right] \tag{29}$$

with boundary conditions

$$\left.\begin{aligned} &\phi^{(1)} = \bar{\phi}^{(1)} = 0 \\ &\frac{1}{r}\frac{\partial \phi^{(1)}}{\partial x} = \frac{1}{r}\frac{\partial \bar{\phi}^{(1)}}{\partial x} = 0 \\ &\frac{\partial}{\partial r}\left(\frac{1}{r}\frac{\partial \phi^{(1)}}{\partial r}\right) = \frac{\partial}{\partial r}\left(\frac{1}{r}\frac{\partial \bar{\phi}^{(1)}}{\partial r}\right) = 0 \end{aligned}\right\} \quad \text{at } r = 0 \tag{30}$$

$$\left.\begin{aligned} &\frac{\partial \phi^{(1)}}{\partial r} = \frac{\partial \bar{\phi}^{(1)}}{\partial r} = 0 \\ &\phi^{(1)} = \bar{\phi}^{(1)} = 0 \end{aligned}\right\} \quad \text{at } r = s \tag{31}$$

Furthermore, by equation (19), equations (9), (10), (13) and (14) become

$$u = -\frac{1}{r}\frac{\partial \phi}{\partial r} = -\frac{1}{r}\frac{\partial}{\partial r}\left(\phi^{(o)} + ke^{iT}\phi^{(o)} + \varepsilon\phi^{(1)} + \varepsilon ke^{It}\phi^{(1)}\right) \tag{32}$$

$$w = \frac{1}{r}\frac{\partial \phi}{\partial x} = \frac{1}{r}\frac{\partial s}{\partial x}\cdot\frac{\partial \phi}{\partial s} = \frac{1}{r}\frac{\partial s}{\partial x}\cdot\frac{\partial}{\partial s}\left(\phi^{(o)} + ke^{iT}\phi^{(o)} + \varepsilon\phi^{(1)} + \varepsilon ke^{It}\phi^{(1)}\right) \tag{33}$$

$$\frac{\partial p}{\partial x} = -\frac{\mathrm{Re}}{\varepsilon}\left[-\frac{1}{r}\frac{\partial^3 \phi^{(o)}}{\partial r^3} + \frac{1}{r^2}\frac{\partial^2 \phi^{(o)}}{\partial r^2} + ke^{iT}\left(-\frac{1}{r}\frac{\partial^3 \bar{\phi}^{(O)}}{\partial r^3} + \frac{1}{r^2}\frac{\partial^2 \bar{\phi}^{(O)}}{\partial r^2}\right)\right] \tag{34}$$

$$\tau_w = -\left(\frac{1}{r}\frac{\partial^2\phi^{(O)}}{\partial r^2} + \frac{1}{r^2}\frac{\partial\phi^{(O)}}{\partial r}\right) - ke^{iT}\left(\frac{1}{r}\frac{\partial^2\bar{\phi}^{(O)}}{\partial r^2} + \frac{1}{r^2}\frac{\partial\bar{\phi}^{(O)}}{\partial r}\right)$$

$$-\varepsilon\left(\frac{1}{r}\frac{\partial^2\phi^{(1)}}{\partial r^2} + \frac{1}{r^2}\frac{\partial\phi^{(1)}}{\partial r}\right) - \varepsilon ke^{iT}\left(\frac{1}{r}\frac{\partial^2\bar{\phi}^{(1)}}{\partial r^2} + \frac{1}{r^2}\frac{\partial\bar{\phi}^{(1)}}{\partial r}\right) \tag{35}$$

The analyses show that the non-steady parts of the solutions are very negligible.

The solutions of equations (20) - (35) are

$$\phi^{(o)} = 2\left(\frac{r}{s}\right)^2 - \left(\frac{r}{s}\right)^4 \tag{36}$$

$$\bar{\phi}^{(o)} = \frac{r^2}{\lambda s^2 I_2(\lambda s)}\left[I_o(\lambda s) - I_o(\lambda r) + I_2(\lambda r)\right] \tag{37}$$

$$\omega^o = -\frac{8}{s^3}\left(\frac{r}{s}\right) \tag{38}$$

$$\bar{\omega}^{(O)} = -2\frac{\lambda I_1(\lambda r)}{s^2 I_2(\lambda s)} \tag{39}$$

$$\phi^{(1)} = -\frac{\mathrm{Re}}{s}\frac{\partial s\varepsilon}{\partial x}\left[\frac{1}{9}\left(\frac{r}{s}\right)^8 - \frac{2}{3}\left(\frac{r}{s}\right)^6 + \left(\frac{r}{s}\right)^4 - \frac{4}{9}\left(\frac{r}{s}\right)^2\right] \tag{40}$$

$$\bar{\phi}^{(1)} = \frac{4\mathrm{Re}}{\lambda^4 s^4}\frac{\partial s}{\partial x}\left\{\frac{I_1(\lambda r)}{s\lambda^2 I_2(\lambda s)}\left[\left(\frac{2}{3}s^4\lambda^4 - 5s^2\lambda^2 - 32\right)\lambda I_1^2(\lambda s)\right.\right.$$

$$+\left(\frac{1}{2}s^2\lambda^2 + 16\right)\lambda^2 s I_o(\lambda s) I_1(\lambda s) + \left(\frac{2}{3}\lambda^4 s^4 + 12\lambda^2 s^2 - 128\right)\frac{I_1(\lambda s)}{s}$$

$$\left.\left. + \left(64 - 6\lambda^2 s^2 - \frac{1}{4}\lambda^4 s^4\right)\lambda I_o(\lambda s)\right]\right\} \tag{41}$$

$$\omega^{(1)} = \frac{8\mathrm{Re}}{s^4}\frac{\partial s}{\partial x}\left[\frac{2}{3}\left(\frac{r}{s}\right)^5 - 2\left(\frac{r}{s}\right)^3 + \left(\frac{r}{s}\right)\right] \tag{42}$$

$$\bar{\omega}^{(1)} = 4\frac{\mathrm{Re}}{\lambda^4 s^4}\frac{\partial s}{\partial x}\left\{\frac{1}{\lambda^2 I^2(\lambda s)}\left[\left(\frac{2s^4\lambda^4}{3} - 5s^2\lambda^2 - 32\right)\lambda I_1^2(\lambda s)\right]\right.$$

$$\left. + \left[I_o(\lambda r)\left(\lambda s^2 r - \frac{\lambda r^2}{3}\right)I_1(\lambda s) - \frac{r^3}{s} + 2sr\right]\right\} \tag{43}$$

$$u = -\frac{4}{s^2} + \frac{4r^2}{s^4} - \frac{ke^{iT}}{\lambda s^2 I_2(\lambda s)}2\left(I_o(\lambda s) - I_o(\lambda r) + \lambda r I_1(\lambda r)\right)$$

$$+ \frac{\varepsilon\,\mathrm{Re}}{s^3}\frac{\partial s}{\partial x}\left[\frac{8}{9}\left(\frac{r}{s}\right)^6 - 4\left(\frac{r}{s}\right)^4 + 4\left(\frac{r}{s}\right)^2 - 18\right]$$

$$+ \frac{\varepsilon k e^{iT}}{r\lambda^4 s^6 I_2(\lambda s)}4\,\mathrm{Re}\frac{\partial s}{\partial x}\left\{\frac{I_o(\lambda r)}{s\lambda I_2(\lambda s)}\left[\begin{array}{l}\left(\frac{2}{3}s^4\lambda^4 - s5^2\lambda^2 - 32\right)\lambda I_1^2(\lambda s) \\ +\left(\frac{1}{2}s^2\lambda^2 + 16\right)\lambda^2 s I_o(\lambda s) \\ +\left(\frac{3}{2}s^4\lambda^4 - 12s^2\lambda^2 - 128\right)\frac{I_1(\lambda s)}{s} \\ +\left(64 - 6s^2\lambda^2 - \frac{1}{4}s^4\lambda^4\right)I_o(\lambda s)\end{array}\right]\right.$$

$$\left. + \lambda^4 r^2\left(\frac{3}{2}s^2 - \frac{8}{\lambda^2}\right)I_1(\lambda r)I_1(\lambda s) - \frac{4}{3}\lambda^3 r^2 I_o(\lambda r)I_1(\lambda s) + ..\right\} \tag{44}$$

$$w = \left(4\frac{r^3}{s^5} - 2\frac{r}{s^3}\right)\frac{\partial s}{\partial x}$$

$$-\frac{ke^{iT}r}{sI_2^2(\lambda s)}\frac{\partial s}{\partial x}\left[I_o(\lambda s)I_1(\lambda s) - I_1(\lambda s)I_o(\lambda r) + I_1(\lambda s)I_2(\lambda r)\right]$$

$$+\varepsilon\frac{\mathrm{Re}}{s^3}\left(\frac{\partial s}{\partial x}\right)^2\left[\left(\frac{r}{s}\right)^7 - \frac{14}{3}\left(\frac{r}{s}\right)^5 + 5\left(\frac{r}{s}\right)^3 - 27\left(\frac{r}{s}\right)\right]$$

$$+\varepsilon k e^{iT}\left\{\begin{array}{l}\dfrac{4\mathrm{Re}}{r\lambda^6}I_2(\lambda r)\dfrac{\partial s}{\partial x}\left[\begin{array}{l}\dfrac{2}{3}\lambda^6\left(2s^3I_o(\lambda s)I_1(\lambda s)I_2^2(\lambda s)+\dfrac{s^2}{\lambda}\left(I_1^2(\lambda s)I_2^2(\lambda s)\right)\right)\\ -5\lambda^4\left(2s^5I_o(\lambda s)I_1(\lambda s)I_2^2(\lambda s)-\dfrac{s^4}{\lambda}I_1^2(\lambda s)I_2^2(\lambda s)\right)\\ -32\lambda^2\left(2s^7I_o(\lambda s)I_1(\lambda s)I_2^2(\lambda s)-3\dfrac{s^6}{\lambda}I_1^2(\lambda s)I_2^2(\lambda s)\right)\end{array}\right]\\ +\dfrac{4\mathrm{Re}r}{s4I_2^2(\lambda s)}I_2(\lambda r)\dfrac{\partial s}{\partial x}\left[\begin{array}{l}I_o(\lambda s)-\dfrac{4}{3s^2}\left(I_o(\lambda s)-\dfrac{2I_1(\lambda s)}{\lambda s}\right)\\ -\dfrac{8}{\lambda^2s^2}\left(I_o(\lambda s)-\dfrac{2I_1(\lambda s)}{\lambda s}\right)\end{array}\right]\end{array}\right\} \quad (45)$$

$$p=\frac{1}{\varepsilon}\left[\frac{36x}{s^4}-\frac{ke^{iT}x}{s^2I_2(\lambda r)}\left[\frac{10}{r}I_1(\lambda r)+7\lambda rI_o(\lambda r)-\left(\lambda^2r+\lambda^2r^2\right)I_1(\lambda r)\right]\right],\quad 0\le x\le 1 \quad (46)$$

$$\tau_w=\frac{8}{s^2}-\frac{ke^{iT}x}{s^2I_2(\lambda s)}\left(\lambda s^2I_o(\lambda s)+4sI_1(\lambda s)\right)+\varepsilon\frac{8}{3s^3}\mathrm{Re}\frac{\partial s}{\partial x}+$$

$$\frac{\varepsilon k e^{iT}}{\lambda^4s^6I_2(\lambda r)}\mathrm{Re}\frac{\partial s}{\partial x}\left\{\begin{array}{l}\dfrac{I_1(\lambda s)}{s^2I_2(\lambda s)}\left[\begin{array}{l}\left(\dfrac{2}{3}s^4\lambda^4-s^2\lambda^2-32\right)I_1^2(\lambda s)\\ +\left(\dfrac{1}{2}s^2\lambda^2+16\right)\lambda^2sI_o(\lambda s)I_1(\lambda s)\\ \left(\dfrac{3}{2}s^4\lambda^4-12s^2\lambda^2-128\right)\dfrac{I_1(\lambda s)}{s}\\ +\left(64-6s^2\lambda^2-\dfrac{1}{4}s^4\lambda^4\right)I_o(\lambda s)\end{array}\right]\\ +\lambda^4\left(\dfrac{4s}{3}-6s^3+\dfrac{32s}{\lambda^2}\right)I_1^2(\lambda s)\end{array}\right\} \quad (47)$$

where $I_o(\lambda r)$, $I_1(\lambda r)$, $I_2(\lambda r)$, $I_o(\lambda s)$, $I_1(\lambda s)$ and $I_2(\lambda s)$ are the modified Bessel function of order zero, one and two, respectively.

Similarly, the geometries under consideration are: the convergent channel $s=e^{-x/2}$, and divergent channel $s=e^{x/2}$.

3 Results and Discussion

The effects of Reynolds number on the flow behaviour of blood in the regions before and after the stenos critical height, and which are approximated as convergent and divergent channels as shown in Fig. 1 of part

one of these studies are considered. The problem shows that the flow structure depends on variation in the Reynolds number. For this, Figs. 1–6 show the computational results for the velocities and wall shear stress for various values of Reynolds number and constant values of other parameters, using Mathematica computational software. For realistic values of $T=\pi/4$, $\lambda=2$, $k=0.03$, $\varepsilon=0.05$, Re 10, 100, 500, 1000 the profiles show that the increase in the Reynolds number produces a commensurate increase in the velocities and wall shear stress.

In the regions before the plague, that is, in the upstream, the flow is laminar, Poiseuille and fully developed. Therefore, the Reynolds number is moderate. But towards the peak of the constriction, that is, in the convergent channel whose geometry narrows down exponentially, the inertial force rises such that the Reynolds number and the momentum increase On the other hand, in the divergent channel whose geometry widens away exponentially from the peak, the inertial force must drop. This must be followed by a drop in the Reynolds number and momentum, and subsequently the velocities and other factors of the flow must drop. This is supposed to be the case in the divergent channel. Therefore, the increase in the velocities and wall shear stress in the divergent channel, possibly, could be due to the influence of the flow situations in the convergent region on it. And, these account for the observations noticed in Figs.1–6.

Furthermore, a flow separation is seen in the radial velocity flow structure at $r \leq 0.3$ in both convergent and divergent regions (see Figs. 2 and 3). This is in consonance with [1], which showed that separation virtually occurs in the flow. The occurrence of this special feature at such point could be due to adverse flow conditions there. According to [1], the flow separation is due to the viscous effects at such point. And, until the point $r \leq 0.3$, where the radial velocity drops to zero, it increases as the Reynolds number increases. After this point, the flow pattern changes such that the velocity decreases as the Reynolds number increases.

More so, the increase in the axial velocity arising from the increase in the Reynolds number tends to cushion the effects of arbitrary increase in the pulse amplitude and height of constriction which decrease the axial velocity.

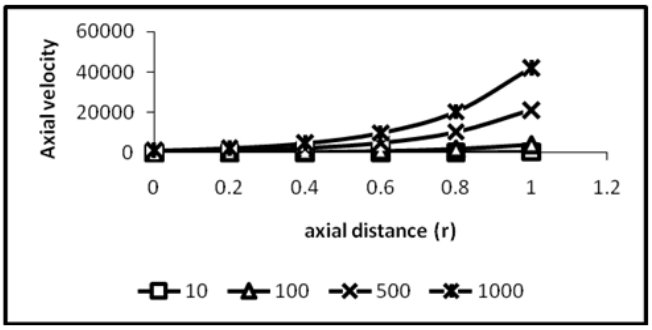

Fig. 1. Axial velocity-Reynolds number profile in a convergent channel

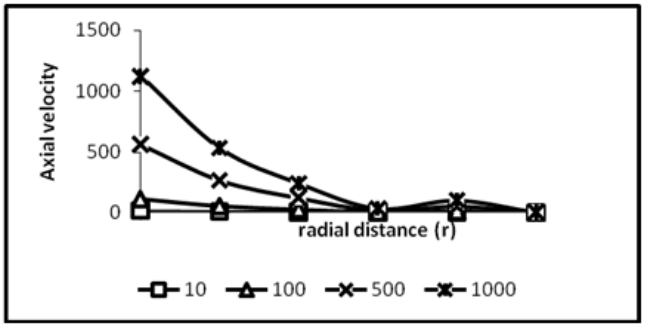

Fig. 2. Axial velocity-Reynolds number profile in a divergent channel

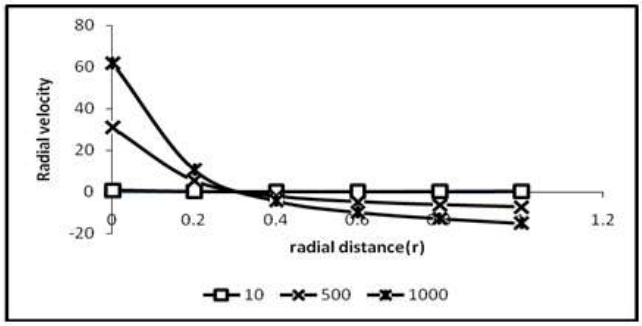

Fig. 3. Radial velocity-Reynolds number in a convergent channel

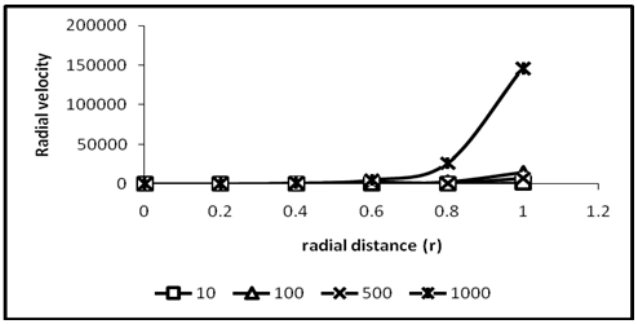

Fig. 4. Radial velocity-Reynolds number profile in a divergent channel

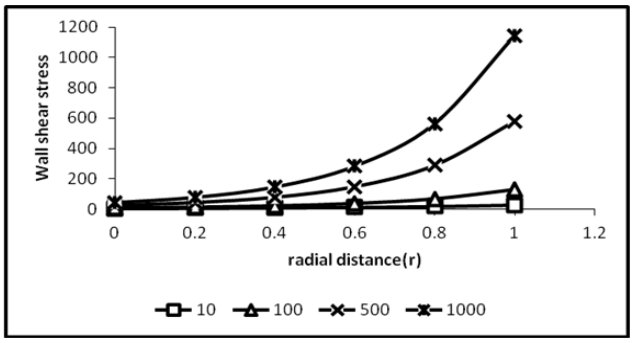

Fig. 5. Wall shear stress-Reynolds number profile in a convergent channel

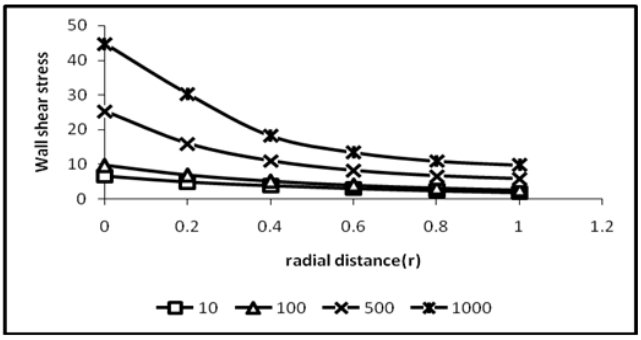

Fig. 6. Wall shear stress-Reynolds number profile in a divergent channel

4 Conclusions

The oscillatory flow of an incompressible viscous fluid through axi-symmetric convergent and divergent channels is examined for the effects of Reynolds number. The overall analysis indicates that the increase in the Reynolds number tends to increase the velocities and wall shear stress. Furthermore, the increase in the axial velocity due to the increase in Reynolds number tends to cushion the adverse effects of pulse amplitude and height of constriction on it.

Acknowledgement

We want to the express our gratitude to the Springer Publishers, who through their Springer Science + Business Media allowed us to adopt the solutions to equations (27) and (29) as expressed in equations (41) and (43) from [1].

Competing Interests

Authors have declared that no competing interests exist.

References

[1] Rao AR, Devanathan R. Pulsatile flow in tubes of varying cross-sections. Z. Angew Maths Physics. 1973;24:203-213.

[2] Burns JC, Parkes T. Flow of incompressible fluid in peristaltic tubes. Journal of Fluid Mechanics. 1967;29:731.

[3] Shapiro AH, Jaffins MY, Weinburg SL. Flow of incompressible fluid in peristaltic tubes. Journal of Fluid Mechanics. 1969;37:409.

[4] Lee JS, Fung YC. Flow of incompressible fluid in locally constricted tubes. Journal of Applied Mechanics. 1970;37:9.

[5] Yin FC, Fung YC. Flow of incompressible fluid in peristaltic tubes. Journal of Applied Mechanics. 1971;47:93.

[6] Creff R, Andrew P. Dynamic and convective results from a developing unsteady flow. International Journal of Numerical Methods in Fluids. 1985;5:745-760.

[7] Haneke H, Laschelfski H, Grobe-Gergemann A, Mitra NK. Natural forced convection and combustion simulation. Advanced Computer Methods in Heat Transfer. 1992;11(2):287-298.

[8] Abraham JP, Sparrow EM, Lovik RD. Unsteady three-dimensional fluid mechanic analysis of blood flow in plaque-narrowed and plaque-free arteries. International Journal of Heat and Mass Transfer. 2008;51:5633-5641.

[9] Sparrow EM, Abraham JP, Minkowycz WJ. Flow separation in a diverging conical duct: Effect of Reynolds number and divergence angle. International Journal of Heat and Mass Transfer. 2009;52:3079-3083.

[10] Gebreegziabher T, Sparrow EM, Abraham JP, Ayorinde E, Singh T. High-frequency pulsatile pipe flows encompassing all flow regimes. Numerical Heat Transfer A. 2011;60:811-826.

[11] Mekheimer KhS, Haroun MH, El Kot MA. Influence of heat and mass transfer in blood flow through an anisotropically tapered and elastic arteries with overlapping stenois. Applied Mathematical Information Science. 2012;6(2):281–292.

[12] Usman M, Naheed Z, Aqsa N. On MHD flow of an incompressible viscous fluid in convergent and divergent channels. Journal of the Egyptian Mathematical Society. 2014;22:214–219.

Peer-review history:
The peer review history for this paper can be accessed here (Please copy paste the total link in your browser address bar)
http://sciencedomain.org/review-history/13476